

1
2
3
4
5
6

Photonic metamaterials: Magnetism at optical frequencies

Stefan Linden, Christian Enkrich, Gunnar Dolling, Matthias W. Klein, Jiangfeng Zhou, Thomas Koschny, Costas M. Soukoulis, Sven Burger, Frank Schmidt, and Martin Wegener

(Invited Paper)

Abstract—Photonic Metamaterials are man-made materials with “lattice constants” smaller than the wavelength of light. Tailoring the properties of their functional building blocks (“atoms”) allows to go beyond the possibilities of usual materials. For example, magnetic dipole moments at optical frequencies ($\mu \neq 1$) become possible. This aspect substantially enriches the possibilities of optics and photonics and forms the basis for so-called negative-index metamaterials. Here, we describe the underlying physics and review the recent progress in this rapidly emerging field.

Index Terms—Metamaterial, split-ring resonator, negative permeability.

I. INTRODUCTION

IN a usual crystal, the atoms are arranged in a periodic fashion with lattice constants on the order of half a nanometer. This is orders of magnitude smaller than the wavelength of light. For example, green light has a wavelength of about 500 nanometers. Thus, for a given direction of propagation, the light field experiences an effective homogeneous medium, that is, it does not “see” the underlying periodicity but only the basic symmetries of the crystal. In such materials, the phase velocity of light c may depend on the propagation direction and is generally different from the vacuum speed of light c_0 by a factor called the refractive index $n = c_0/c$ (the slowness). The physical origin are microscopic electric dipoles that are excited by the electric field component of the incoming light and that radiate with a certain retardation. Hence, the electric permittivity is different from unity, i.e., $\epsilon \neq 1$. In contrast to this, magnetic dipoles play no role at optical frequencies in natural substances, i.e., the magnetic permeability is unity, $\mu = 1$.

Electromagnetic metamaterials are artificial structures with inter-“atomic” distances (or “lattice constants”) that are still

smaller than the wavelength of light. Similarly, the light field “sees” an effective homogeneous material for any given propagation direction (quite unlike in a Photonic Crystal). The building blocks (“atoms”), however, are not real atoms but are rather made of many actual atoms, often metallic ones. It is this design aspect that allows us to tailor the electromagnetic material properties, in particular the corresponding dispersion relation, to a previously unprecedented degree. For example, it becomes possible to achieve magnetic dipole moments at optical frequencies, i.e., magnetism at optical frequencies ($\mu \neq 1$). It turns out that, for $\epsilon < 0$ and $\mu < 0$, the refractive index becomes negative with $n = -\sqrt{\epsilon\mu} < 0$ (rather than $n = +\sqrt{\epsilon\mu} > 0$). This aspect was pointed out by Veselago many years ago [1], but remained an obscurity until rather recently.

In this review, we first describe the physics of “magnetic atoms” (e.g. so called split-ring resonators), which can be best viewed as the magnetic counterpart of the famous Lorentz oscillator model for electric dipoles in optical materials. By simple size scaling, these concepts have recently been brought towards the optical regime. We also discuss the limits of size scaling. Alternative “magnetic atom” designs can push the limits somewhat further and can also ease nanofabrication of these metamaterials.

II. PHYSICS OF SPLIT-RING RESONATORS AS “MAGNETIC ATOMS”

It is well-known from basic magnetostatics that a magnetic dipole moment can be realized by the circulating ring current of a microscopic coil, which leads to an individual magnetic moment given by the product of current and area of the coil. This dipole moment vector is directed perpendicular to the plane of the coil. If such a coil is combined with a plate capacitor, one expects an increased current at a finite-frequency resonance, hence an increased magnetic dipole moment. Thus, a popular design for magnetic “atoms” is to mimic a usual LC -circuit, consisting of a plate capacitor with capacitance C and a magnetic coil with inductance L , on a scale much smaller than the relevant wavelength of light.

Figure 1 shows the analogy of a conventional LC circuit and a metallic split-ring resonator (SRR) on a dielectric surface. The RHS shows an electron micrograph of a single gold SRR fabricated by standard electron-beam lithography. The name “split-ring resonator” goes back to the 1981 work of Hardy and Whitehead [2] and that of Pendry from 1999 [3].

S. Linden and M. Wegener are with Institut für Nanotechnologie, Forschungszentrum Karlsruhe in der Helmholtz-Gemeinschaft, D-76021 Karlsruhe, Germany

C. Enkrich, G. Dolling, M.W. Klein, and M. Wegener are with Institut für Angewandte Physik, Universität Karlsruhe (TH), D-76131 Karlsruhe, Germany

J.F. Zhou, Th. Koschny, and C.M. Soukoulis are with Ames Laboratory and Department of Physics and Astronomy, Iowa State University, Ames, Iowa 50011, U.S.A.

Th. Koschny and C.M. Soukoulis are with Institute of Electronic Structure and Laser, FORTH, 71110 Heraklion, Crete, Greece

C.M. Soukoulis is with Department of Materials Science and Technology, 71110 Heraklion, Crete, Greece

S. Burger and F. Schmidt are with Zuse Institute Berlin, Takustraße 7, D-14195 Berlin, Germany and DFG Forschungszentrum MATHEON, Straße des 17. Juni 136, 10623 Berlin, Germany

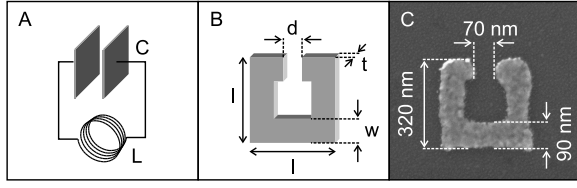


Fig. 1. Illustration of the analogy between a usual LC circuit, A, and a split-ring resonator (SRR), B. The electron micrograph in C shows an actually fabricated structure, a gold SRR ($t = 20$ nm) on a glass substrate. Taken from [6].

This name shall be employed below. However, the SRR has also previously been discussed under the names “slotted-tube resonator” in 1977 [4] in the context of nuclear magnetic resonance (NMR) and “loop-gap resonator” in 1996 [5].

The position of the anticipated LC -resonance frequency can be estimated by the following crude approach: Suppose that we can describe the capacitance by the usual textbook formula for a large capacitor with nearby plates ($C \propto \text{plate area/distance}$) and the inductance by the formula for a “long” coil with N windings for $N = 1$ ($L \propto \text{coil area/length}$). Using the nomenclature of Fig. 1 B, i.e., the width of the metal w , the gap size of the capacitor d , the metal thickness t , and the width of the coil l , we get

$$C = \epsilon_0 \epsilon_C \frac{wt}{d}, \quad (1)$$

with the relative permittivity of the material in between the plates ϵ_C , and

$$L = \mu_0 \frac{l^2}{t}. \quad (2)$$

This leads to the eigenfrequency

$$\omega_{LC} = \frac{1}{\sqrt{LC}} = \frac{1}{l} \frac{c_0}{\sqrt{\epsilon_C}} \sqrt{\frac{d}{w}} \propto \frac{1}{\text{size}}, \quad (3)$$

and to the LC -resonance wavelength

$$\lambda_{LC} = \frac{2\pi c_0}{\omega_{LC}} = l 2\pi \sqrt{\epsilon_C} \sqrt{\frac{w}{d}} \propto \text{size}. \quad (4)$$

Despite its simplicity and the crudeness of our derivation, this formula contains a lot of correct physics, as confirmed by numerical calculations (see below): First, it tells us that the LC -resonance wavelength is proportional to the linear dimension of the coil l , provided that the ratio w/d is fixed. This scaling is valid as long as the metal actually behaves like a metal, i.e., as long as the LC resonance frequency is much smaller than the metal plasma frequency ω_{pl} . We will come back to this fundamental limitation below. Second, for relevant parameters ($\epsilon_C \geq 1$ and $w \approx d$), the prefactor is typically on the order of ten, i.e.,

$$\lambda_{LC} \approx 10 \times l. \quad (5)$$

Thus, it is possible to arrange these SRRs in the form of an array in the xy -plane such that the lattice constant a_{xy} is much smaller than the resonance wavelength, i.e., $a_{xy} \ll \lambda_{LC}$. For example: For a telecommunication wavelength of $\lambda_{LC} = 1.5 \mu\text{m}$, the linear dimension of the coil would need to be on

the order of $l = 150$ nm, implying minimum feature sizes around 50 nm or yet smaller. Under these conditions, typical values for the capacitance and the inductance are $C \approx 1$ aF and $L \approx 1$ pH, respectively. Third, the dielectric environment influences the resonance via ϵ_C , which is, e.g., modified by the presence of a dielectric substrate. Fourth, if one closes the gap, i.e., in the limit $d \rightarrow 0$ or $C \rightarrow \infty$, the resonance wavelength goes to infinity, or equivalently, the resonance frequency ω_{LC} becomes zero.

What are the limits of size scaling according to Eq.(3)? This question has recently been addressed in Ref. [7]: For an ideal metal, i.e., for an infinite electron density n_e , hence an infinite metal plasma frequency, a finite current I flowing through the inductance is connected with zero electron velocity, hence with a vanishing electron kinetic energy. In contrast, for a real metal, i.e., for a finite electron density, the current is inherently connected with a finite electron velocity v_e . Thus, one must not only provide the usual magnetic energy $\frac{1}{2}LI^2$ to support the current I , but additionally the total electron kinetic energy $N_e \frac{m_e}{2} v_e^2$, where $N_e = n_e V$ is the number of electrons in the SRR contributing to the current. To conveniently incorporate this kinetic energy term into our electromagnetic formulation, we recast it into the form of an additional magnetic energy. Using $n_e e v_e = I/(wt)$ and the volume (=cross section times length) of the SRR wire $V = (wt)(4(l-w)-d)$, we obtain

$$E_{\text{kin}} = N_e \frac{m_e}{2} v_e^2 = \frac{1}{2} L_{\text{kin}} I^2. \quad (6)$$

Here we have introduced the “kinetic inductance”

$$L_{\text{kin}} = \frac{m_e}{n_e e^2} \frac{4(l-w)-d}{wt} \propto \frac{1}{\text{size}}. \quad (7)$$

While the usual inductance L is proportional to the SRR size [see (2)], the kinetic inductance (7) scales inversely with size – provided that all SRR dimensions are scaled down simultaneously. Thus, the kinetic inductance is totally irrelevant for macroscopic coils but becomes dominant for microscopic inductances, i.e., when approaching optical frequencies. The kinetic inductance adds to the usual inductance, $L \rightarrow L + L_{\text{kin}}$ in (3), and we immediately obtain the modified scaling for the magnetic resonance frequency

$$\omega_{LC} \propto \frac{1}{\sqrt{\text{size}^2 + \text{const.}}}. \quad (8)$$

Obviously, the magnetic resonance frequency is inversely proportional to size for a large SRR, whereas it approaches a constant for a small SRR. To evaluate this constant and in order to be simple, we consider the limits $w \ll l$, $d \ll 4l$ and a capacitance C according to (1) in air. Inserting the metal plasma frequency $\omega_{\text{pl}} = \sqrt{(n_e e^2)/(\epsilon_0 m_e)}$, we obtain the maximum magnetic resonance frequency

$$\omega_{LC}^{\text{max}} = \sqrt{\frac{1}{L_{\text{kin}} C}} = \omega_{\text{pl}} \sqrt{\frac{d}{4l}}. \quad (9)$$

This saturation frequency is further reduced by the dielectric environment and by the skin effect [7], which we have tacitly neglected in our simple reasoning. Furthermore, we remind that our results are implicitly based on the Drude model of

metal *intraband* transitions. For real metals in the optical regime, *interband* transitions often play a significant role as well. Our results are only meaningful if ω_{LC}^{\max} is smaller than the onset frequency of interband transitions. For example, interband transitions occur for wavelengths below 800 nm (550 nm) in aluminum (gold).

One can even obtain an explicit and simple expression for the magnetic permeability $\mu(\omega)$ from our simple circuit reasoning. We start by considering an excitation configuration where the electric-field component of the light cannot couple to the SRR (see below) and where the magnetic field is normal to the SRR plane. Under these conditions, the self-induction voltage of the inductance L plus the voltage drop over the capacitance C equals the voltage U_{ind} induced by the *external* magnetic field, i.e., $U_L + U_C = U_{\text{ind}}$ or

$$L \dot{I} + \frac{1}{C} \int I dt = U_{\text{ind}} = -\dot{\phi}. \quad (10)$$

Again assuming a homogeneous magnetic field in the coil, we obtain the external magnetic flux $\phi = l^2 \mu_0 H$, with the external magnetic field $H = H_0 e^{-i\omega t} + \text{c.c.}$ Taking the time derivative of (10) and dividing by L yields

$$\ddot{I} + \frac{1}{LC} I = \frac{1}{L} \dot{U}_{\text{ind}} = +\omega^2 \frac{\mu_0 l^2}{L} H_0 e^{-i\omega t} + \text{c.c.} \quad (11)$$

Upon inserting the obvious ansatz $I = I_0 e^{-i\omega t} + \text{c.c.}$, we obtain the current I , the individual magnetic dipole moment $l^2 I$, and the magnetization $M = (N_{LC}/V) l^2 I$. Here we have introduced the number of LC circuits N_{LC} per volume V . Suppose that the lattice constant in the SRR plane is $a_{xy} \geq l$, and $a_z \geq t$ in the direction normal to the SRRs. This leads to $N_{LC}/V = 1/(a_{xy}^2 a_z)$. Finally using $M = \chi_m(\omega) H$, $\mu(\omega) = 1 + \chi_m(\omega)$, and (2) brings us to

$$\mu(\omega) = 1 + \frac{\mathcal{F} \omega^2}{\omega_{LC}^2 - \omega^2}. \quad (12)$$

Apart from the $\propto \omega^2$ numerator, this represents a Lorentz-oscillator resonance. Here we have lumped the various prefactors into the dimensionless quantity \mathcal{F} with

$$0 \leq \mathcal{F} = \frac{l^2 t}{a_{xy}^2 a_z} \leq 1. \quad (13)$$

$\mathcal{F} = 1$ corresponds to nearest-neighbor SRRs touching each other – obviously the ultimate upper bound for the accessible SRR density. Thus, we can interpret \mathcal{F} as a filling fraction. Ohmic losses, radiation losses and other broadening mechanisms can be lumped into a damping γ_m of the magnetic resonance.

The bottom line is that the split-ring resonator is the magnetic analogue of the usual (electric) Lorentz oscillator model. The permeability of a closed ring, i.e., the special case of $d \rightarrow 0 \Rightarrow C \rightarrow \infty \Rightarrow \omega_{LC} \rightarrow 0$ in (12), reduces to

$$\mu(\omega) = \text{const.} = 1 - \mathcal{F} \geq 0. \quad (14)$$

In other words: The split in the ring is *essential* for obtaining $\mu(\omega) < 0$. For example, for 30% lateral spacing ($a_{xy} = 1.3 \times l$)

and for a spacing in the vertical direction equal to the SRR thickness ($a_z = 2 \times t$), we obtain $\mathcal{F} = 0.30$ and $\mu = 0.70$ for closed rings. Note, however, that we have tacitly neglected the interaction among the rings in our considerations leading to this conclusion. The assumption of noninteracting rings is justified for $\mathcal{F} \ll 1$, but becomes questionable for $\mathcal{F} \rightarrow 1$. What qualitative modifications are expected from the interaction of rings? The fringing field of any particular ring at the location of its in-plane neighbors is opposite to its own magnetic dipole moment, hence parallel to the external magnetic field of the light. Thus, in-plane interaction tends to effectively increase the value of \mathcal{F} in (14). In contrast, interaction with rings from adjacent parallel planes tends to suppress \mathcal{F} in (14). It is presently unclear, whether a particular arrangement of rings could allow for an increase of \mathcal{F} sufficient to obtain $\mu(\omega) < 0$ (also see Ref. [3]). Interaction similarly influences the behavior of split rings.

We note in passing that the description of an isotropic (meta)material in terms of $\epsilon(\omega)$ and $\mu(\omega)$ may be valid, but it is not unique. Indeed, it has already been pointed out in Ref. [8] that, alternatively, one can set $\tilde{\mu} = 1$ and describe the (meta)material response in terms of *spatial dispersion*, i.e., via a wave-vector dependence of the electric permittivity $\tilde{\epsilon}(\omega, k)$. One must be aware, however, that the resulting “refractive index” $\tilde{n}(\omega, k)$ loses its usual meaning. A more detailed discussion of this aspect can be found in Ref. [9].

Historically, the first demonstration of negative-index metamaterials was in 2001 at around 10 GHz frequency or 3 cm wavelength [10], a regime in which SRR “magnetic atoms” can easily be fabricated on electronic circuit boards. The negative permittivity was achieved by additional metal stripes. In 2004 [11], $\mu(\omega) < 0$ has been demonstrated at about 1 THz frequency (300 μm wavelength) using standard microfabrication techniques for the SRR. Ref. [12] reviews this early work.

III. TOWARDS MAGNETISM AT OPTICAL FREQUENCIES

At this point, our experimental team entered this field – partly driven by the scepticism that similar materials would *not* be possible at optical frequencies. In our first set of experiments, we scaled down the lateral size of the SRR by two more orders of magnitude, leading to the following parameters: $l = 320 \text{ nm}$, $w = 90 \text{ nm}$, $t = 20 \text{ nm}$, and $d = 70 \text{ nm}$. On this basis, we anticipated a magnetic resonance at about $\lambda_{LC} = 3 \mu\text{m}$ wavelength. These “magnetic atoms” were arranged on a square lattice with $a_{xy} = 450 \text{ nm} \approx 7 \times \lambda_{LC}$ (and larger ones) and a total sample area of $(25 \mu\text{m})^2$. For normal incidence conditions, however, the light has zero magnetic-field component perpendicular to the SRR plane. Thus, excitation via the magnetic field is not possible. Alternatively, the magnetic resonance can also be excited via the electric-field component of the light if it has a component normal to the plates of the capacitor, i.e., if the incident light polarization is horizontal. In contrast, for normal incidence and vertical incident polarization, neither the electric nor the magnetic field can couple to the SRR. This “selection rule” can be used to unambiguously identify the magnetic resonance.

Corresponding measured transmittance and reflectance spectra are shown in Fig. 2. Independent of the lattice constant, a_{xy} ,

two distinct resonances are clearly visible. With increasing a_{xy} , these resonances narrow to some extent because of the reduced interaction between the SRRs, but their spectral position remains essentially unchanged as expected for the electric and magnetic resonant responses of SRRs. This also clearly shows that Bragg diffraction plays no major role. The long-wavelength resonance around $3\mu\text{m}$ wavelength is present for horizontal incident polarization and absent for vertical polarization – as expected from the above reasoning. Furthermore, as expected from the previous section, this resonance disappears for closed rings (Fig. 2 G and H), i.e., for $d \rightarrow 0$, hence $\omega_{LC} \rightarrow 0$. The additional short-wavelength resonance between 1 and $2\mu\text{m}$ wavelength is due to the particle plasmon or Mie resonance, mainly exhibiting an electric permittivity, which follows a Lorentz oscillator form according to

$$\epsilon(\omega) = 1 + \frac{\mathcal{F} \omega_{\text{pl}}^2}{\omega_{\text{Mie}}^2 - \omega^2 - i\gamma\omega}, \quad (15)$$

with the metal Drude model damping γ . The constant \mathcal{F} depends on the SRR volume filling fraction. We will come back to the Mie resonance in more detail below.

All features of the measured spectra (Fig. 2) are reproduced by numerical calculations using a three-dimensional finite-difference time-domain approach [6] (not shown here). The corresponding calculated field distributions [6] (not shown here) support the simplistic reasoning on SRRs in the previous section. Retrieving [13] the effective permittivity $\epsilon(\omega)$ and magnetic permeability $\mu(\omega)$ from the calculated spectra, indeed reveals $\mu < 0$ associated with the $\lambda_{LC} = 3\mu\text{m}$ resonance for appropriate polarization conditions [6].

Two questions immediately arise: (i) Can the magnetic resonance frequency be further increased by miniaturization of the SRRs and (ii) can one also experimentally demonstrate coupling to the magnetic (or LC) resonance via the magnetic-field component of the light at optical frequencies? Both aspects have been addressed in our Ref. [14]. Electron micrographs of miniaturized structures are shown in Fig. 3 (a). (i) The corresponding measured spectra for horizontal incident polarization in Fig. 3 (b) reveal the same (but blue-shifted) resonances as in Fig. 2 A. For vertical incident polarization, compare Fig. 3 (c) and Fig. 2 B. (ii) In Fig. 4(a), the electric component of the incident light can not couple to the LC circuit resonance for any angle [in (b) it can]. With increasing angle, however, the magnetic field acquires a component normal to the SRR plane. This component can induce a circulating electric current in the SRR coil via the induction law. This current again leads to a magnetic dipole moment normal to the SRR plane, which can counteract the external magnetic field. The magnitude of this resonance (highlighted by the gray area around $1.5\mu\text{m}$ wavelength) is indeed consistent with theory [14] (not depicted here) and leads to an effective negative magnetic permeability for propagation in the SRR plane and for a stack of SRR layers rather than just one layer as considered here. This aspect has been verified explicitly by retrieving the effective permittivity and permeability from the calculated transmittance and reflectance spectra [13], [15].

An unexpected feature of the spectra in Fig. 4 (a) is that the 950-nm wavelength Mie resonance at normal incidence

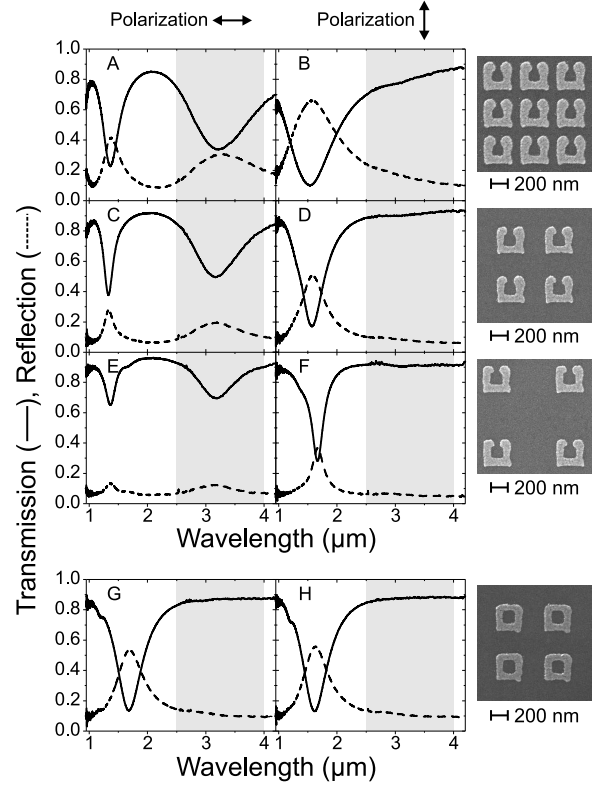


Fig. 2. Measured transmittance and reflectance spectra (normal incidence). In each row of this “matrix”, an electron micrograph of the corresponding sample is shown on the RHS. The two polarization configurations are shown on top of the two columns. A, B (lattice constant $a = 450\text{ nm}$), C, D ($a = 600\text{ nm}$) and E, F ($a = 900\text{ nm}$) correspond to nominally identical split-ring resonators, G and H ($a = 600\text{ nm}$) to corresponding closed rings. The combination of these spectra unambiguously shows that the resonance at about $3\mu\text{m}$ wavelength (highlighted by the gray areas) is the LC resonance of the individual split-ring resonators. Taken from [6].

splits into two resonances for oblique incidence. This aspect is reproduced by numerical calculations [14], [16]. Intuitively, it can be understood as follows: For normal incidence and vertical polarization, the two similarly shaped vertical SRR arms contribute. These arms are coupled via the SRR’s bottom arm (and via the radiation field). As usual, the coupling of two degenerate modes leads to an avoided crossing with two new effective oscillation modes, a symmetric and an anti-symmetric one, which are frequency down-shifted and up-shifted as compared to the uncoupled resonances, respectively. The anti-symmetric mode cannot be excited at all for normal incidence as it has zero effective electric dipole moment. The red-shifted symmetric mode can be excited. It even has a larger effective electric dipole moment than a single arm. Indeed, the Mie resonance for vertical polarization is deeper and spectrally broader than for horizontal polarization in Fig. 2, and red-shifted with respect to it. For finite angles of incidence, the phase fronts of the electric field are tilted with respect to the SRR plane. Thus, the vertical SRR arms are excited with a small but finite time delay, equivalent to a finite phase shift. This shift allows coupling to the anti-symmetric mode of the coupled system of the two vertical arms as well. In one half cycle of light, one gets a positive charge at the lower LHS corner of the SRR and a negative charge at the

lower RHS corner, resulting in a compensating current in the horizontal bottom arm. Characteristic snapshots of the current distributions in the SRR have been shown schematically in [14].

According to this reasoning for oblique incidence (e.g., 60°), we expect a circulating current component for wavelengths near the two magnetic resonances at $1.5\mu\text{m}$ and 800nm , respectively. Any circulating current is evidently connected with a current in the horizontal bottom arm of the SRR. According to the usual laws of a Hertz dipole, the corresponding charge oscillation in the bottom arm can radiate into the forward direction with an electric field component orthogonal to the incident polarization. In other words: For oblique incidence, the fingerprint of the magnetic resonances is a rotation of polarization. Such rotation is indeed unambiguously observed in the numerical simulations (not shown here, see [14]) and in the experiments [see grey area in Fig. 4 (a)].

Further down-scaling of the SRR size is eventually limited by the fact that the resonances stop shifting with decreasing SRR size (see discussion in section II). The shortest magnetic resonance wavelengths that we have achieved are around 900nm using gold SRR (not shown, unpublished).

We note in passing that there is a continuous transition between the two-fold degenerate Mie resonance of a metallic square-shaped “particle” and a SRR, exhibiting a magnetic resonance and a Mie resonance. This transition has been investigated by us in Ref. [17] using the rapid prototyping capabilities of focused-ion-beam writing.

The above discussion on the antisymmetric and symmetric eigenmodes of the two coupled vertical SRR arms makes one wonder whether the SRR bottom arm is necessary at all. Indeed, it is not. This has basically been explained above and can alternatively be discussed as follows: Eliminating the bottom arm can be viewed as introducing a second capacitance into the LC -circuit. This effectively reduces the total capacitance in the circuit, hence it increases the magnetic resonance frequency for a given minimum feature size. On the one hand, this eases access to the (near-)visible regime at reduced fabrication effort. On the other hand, this increased resonance frequency at fixed lattice constant decreases the ratio between (resonance) wavelength, λ_{LC} , and lattice constant, a_{xy} , to about $\lambda_{LC}/a_{xy} \approx 2-3$. In the true metamaterial limit, one aims at $\lambda_{LC}/a_{xy} \gg 1$. Recall that the Bragg condition corresponds to $\lambda_{LC}/a_{xy} = 2$. Another significant difference between the original planar SRR design and the resulting cut-wire pairs is that the latter can be rotated by 90 degrees with respect to the substrate. This not only further eases nanofabrication but also allows for a magnetic permeability $\mu(\omega)$ for normal incidence conditions (i.e., the magnetic field can be perpendicular to the plane spanned by the two wire pieces, i.e., parallel to the magnetic dipole moment vector). Corresponding theoretical [18]–[20] and experimental [21]–[23] work has been published.

Figure 5 (a)–(c) shows our results for cut-wire pairs of different length but fixed magnesium fluoride (MgF_2) spacer thickness and fixed gold wire width. The dotted curves in (a) correspond to a nominally identical sample, however, *without*

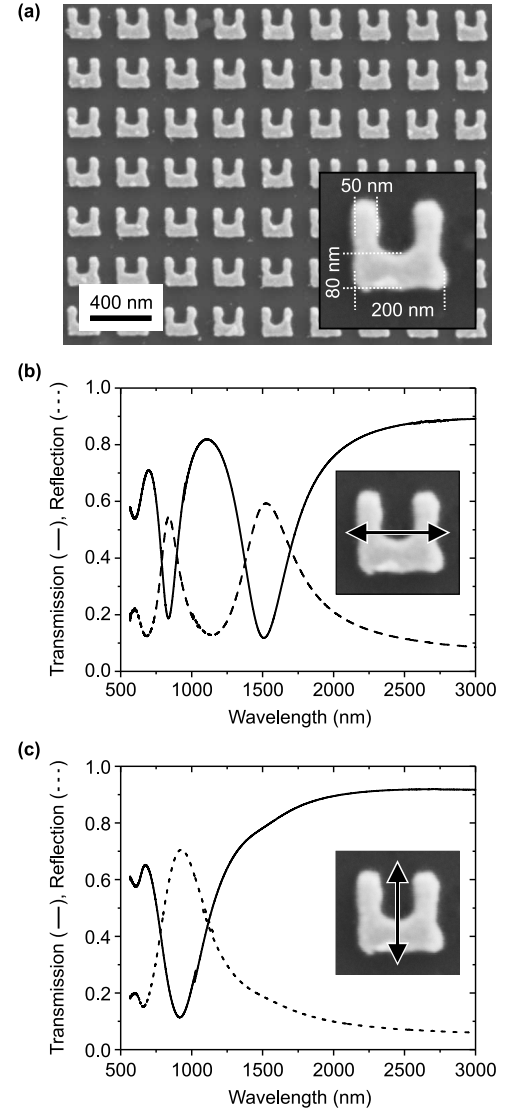


Fig. 3. (a) Electron micrograph of a split-ring array with a total area of $(100\mu\text{m})^2$. The lower RHS inset shows the dimensions of an individual split ring. The corresponding measured normal-incidence transmittance and reflectance spectra for horizontal and vertical polarization are shown in (b) and (c), respectively. Taken from [14].

the upmost gold layer. This single cut-wire sample shows only *one* pronounced resonance – the Mie resonance – for each polarization. For an incident polarization along the long axis of the cut-wire pairs, however, *two* resonances are observed which essentially disappear for orthogonal polarization. A comparison of Fig. 5 (b) and (d) shows the dependence on the MgF_2 spacer thickness d . As expected from the above picture of two coupled oscillators, the splitting between the two effective resonances depends on their coupling: For thin (thick) spacers, the coupling is strong (weak), hence the two resonances are split by a large (small) amount in the spectrum. The obvious polarization dependence of the cut-wire pairs may be undesired in certain cases. Thus, it is interesting to also investigate samples for which the wire width equals the wire length, i.e., where $w = l$. In this case, the cut-wire pairs turn into nanoscopic plate pairs. Their measured optical

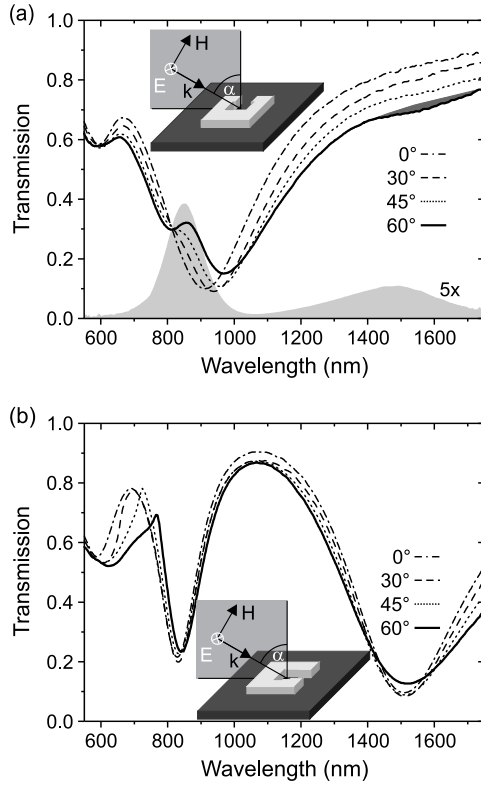


Fig. 4. Measured transmittance spectra taken for oblique incidence for the configurations shown as insets (where $\alpha = 60^\circ$). In (a), coupling to the fundamental magnetic mode at $1.5\mu\text{m}$ wavelength is only possible via the magnetic-field component of the incident light, for (b), both electric and magnetic field can couple. Note the small but significant feature in (a) for 60° around $1.5\mu\text{m}$ wavelength. The lower gray area in (a) is the transmittance into the linear polarization orthogonal to the incident one for $\alpha = 60^\circ$. This observable can be viewed as a fingerprint of magnetic resonances under these conditions. Taken from [14].

properties (shown in Ref. [22]) are qualitatively similar, yet even more pronounced than in the case of cut-wire pairs. Reducing the value of $w = l$, allows for tuning of the resulting resonance positions. The retrieval of $\epsilon(\omega)$ and $\mu(\omega)$ from the calculated spectra corresponding to these parameters yields a negative $\mu(\omega)$ around one micrometer wavelength [22] (not shown). Other groups have even reported a negative real part of the refractive index around $1.5\mu\text{m}$ wavelength for the above cut-wire pair structures [23], as deduced from measured interferometric transmittance and reflectance spectra.

IV. CONCLUSION

In contrast to “conventional textbook wisdom,” the magnetic permeability μ is no longer unity for all optical materials. While $\mu = 1$ holds indeed for all known natural materials at optical frequencies, for metamaterials $\mu \neq 1$ and even $\mu < 0$ can result. In this class of tailored (mostly periodic) structures, split-ring resonators (and variations thereof) play the role of “magnetic atoms” and can lead to local magnetic dipole moments. Thus, split-ring resonators can be viewed as the magnetic counterpart of the famous Lorentz oscillator model for electric dipole moments. For split-ring resonators made from gold, $\mu < 0$ can be achieved at telecommunication wavelengths but not in the visible. Other metals and/or other

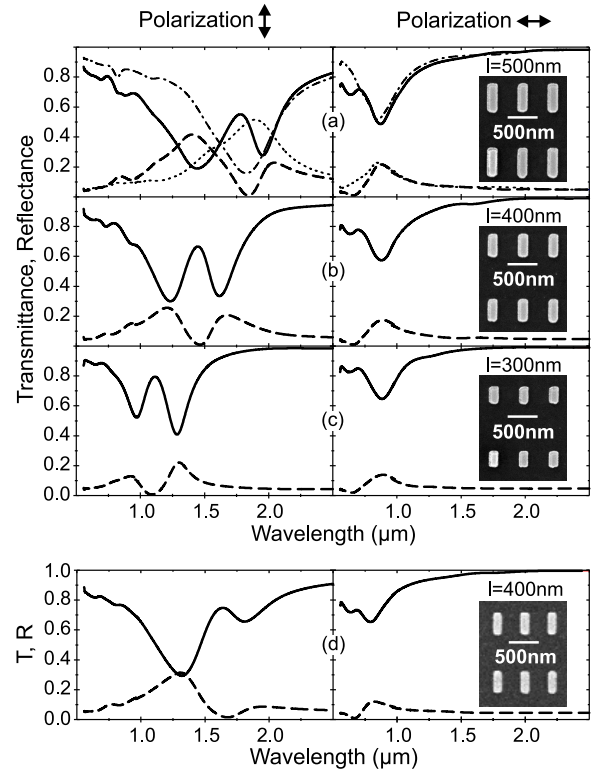


Fig. 5. Measured spectra of transmittance (solid lines) and reflectance (dashed lines) for cut-wire pairs with vertical incident polarization (LHS column) and horizontal polarization (RHS column). Parameters varied: (a) $l = 500\text{ nm}$, (b) $l = 400\text{ nm}$, and (c) $l = 300\text{ nm}$. Fixed parameters for (a)–(c): $w = 150\text{ nm}$, $t = 20\text{ nm}$, $d = 80\text{ nm}$, $a_x = 500\text{ nm}$, and $a_y = 1050\text{ nm}$. The dash-dotted curves in (a) are spectra from a nominally identical structure, but without the upmost gold wire. (d) as (b), but $d = 60\text{ nm}$ rather than 80 nm . The insets in (a)–(d) show corresponding electron micrographs (top view). Taken from [22].

designs might allow for resonances with $\mu < 0$ even in the visible range. Ultimately, the constituent metal plasma frequency sets a fundamental limit.

Where does this field go? Many researchers in the field are driven by the perspective to obtain a negative refractive index n at near-infrared or optical frequencies by combining “magnetic atoms” with $\mu < 0$ and “electric atoms” with $\epsilon < 0$. Indeed, corresponding experiments have been presented very recently [24]. Their figure-of-merit (i.e., the ratio between real and imaginary part of n at frequencies where the real part of n is negative), however, is still below unity, hence not really satisfactory. Improved designs have been proposed theoretically [25]. The search for a negative real part of n itself is driven by the fascinating possibility of a “perfect lens” [26] providing sub-wavelength resolution. Accounting for the “granularity” of metamaterials and deviations from the strict case of $n = -1$ due to the real [27] and/or the imaginary [28] part of n , however, appear to limit “perfect lenses” to very specialized near-field optical configurations.

Possibly, the real potential of photonic metamaterials lies in other unexplored areas, for example in chiral metamaterials or in nonlinear metamaterials. In any case, given today’s possibilities regarding the nanofabrication of tailored “atoms,” only our own imagination and creativity set the limits.

ACKNOWLEDGMENT

We acknowledge support by the Deutsche Forschungsgemeinschaft (DFG) and the State of Baden-Württemberg through the DFG-Center for Functional Nanostructures (CFN) within subprojects A1.4 and A1.5. The research of M.W. is further supported by project DFG-We 1497/9-1, that of C. M. S. by the Alexander von Humboldt senior-scientist award 2002, by Ames Laboratory (Contract No. W-7405-Eng-82), EU FET project DALHM and DARPA (Contract No. HR0011-05-C-0068).

REFERENCES

- [1] V. G. Veselago, "The electrodynamics of substances with simultaneously negative values of ϵ and μ ," *Sov. Phys. Usp.*, vol. 10, no. 4, pp. 509–514, 1968.
- [2] W. N. Hardy and L. A. Whitehead, "Split-ring resonator for use in magnetic resonance from 200–2000 MHz," *Rev. Sci. Instrum.*, vol. 52, no. 2, pp. 213–216, 1981.
- [3] J. B. Pendry and A. J. Holden and D. J. Robbins and W. J. Stewart, "Magnetism from conductors and enhanced nonlinear phenomena," *IEEE Trans. MTT*, vol. 47, no. 14, pp. 2075–2084, 1999.
- [4] H. J. Schneider and P. Dullenkopf, "Slotted tube resonator: A new NMR probe head at high observing frequencies," *Rev. Sci. Instrum.*, vol. 48, no. 1, pp. 68–73, 1977.
- [5] B. T. Ghim, G. A. Rinard, W. Quine, S. S. Eaton, and G. R. Eaton, "Design and fabrication of copper-film loopgap resonators," *J. of Magn. Res. A*, vol. 120, no. 1, pp. 72–76, 1996.
- [6] S. Linden, C. Enkrich, M. Wegener, J. F. Zhou, T. Koschny, and C. M. Soukoulis, "Magnetic response of metamaterials at 100 Terahertz," *Science*, vol. 306, no. 5700, pp. 1351–1353, 2004.
- [7] J. F. Zhou, T. Koschny, M. Kafesaki, E. N. Economou, J. B. Pendry, and C. M. Soukoulis, "Saturation of the magnetic response of split-ring resonators at optical frequencies," *Phys. Rev. Lett.*, vol. 95, pp. 223 902–4, 2005.
- [8] L. D. Landau and E. L. Lifshitz, *Electrodynamics of continuous media*, 2nd edition. New York: Pergamon Press, 1960.
- [9] K. Busch, G. von Freymann, S. Linden, L. Tkeshelashvili, S. Mingaleev, and M. Wegener, "Periodic nanostructures for photonics," *Phys. Rep.*, 2006.
- [10] R. A. Shelby, D. R. Smith, and S. Schultz, "Experimental verification of a negative index of refraction," *Science*, vol. 292, no. 5514, pp. 77–79, 2001.
- [11] T. J. Yen, W. J. Padilla, N. Fang, D. C. Vier, D. R. Smith, J. B. Pendry, D. N. Basov, and X. Zhang, "Terahertz magnetic response from artificial materials," *Science*, vol. 303, no. 5663, pp. 1494–1496, 2004.
- [12] D. R. Smith, J. B. Pendry, and M. C. K. Wiltshire, "Metamaterials and negative refractive index," *Science*, vol. 305, no. 5685, pp. 788–792, 2004.
- [13] D. R. Smith, S. Schultz, P. Markos, and C. M. Soukoulis, "Determination of effective permittivity and permeability of metamaterials from reflection and transmission coefficients," *Phys. Rev. B*, vol. 65, no. 19, pp. 195 104–5, 2002. [Online]. Available: <http://link.aps.org/abstract/PRB/v65/e195104>
- [14] C. Enkrich, M. Wegener, S. Linden, S. Burger, L. Zschiedrich, F. Schmidt, J. F. Zhou, T. Koschny, and C. M. Soukoulis, "Magnetic metamaterials at telecommunication and visible frequencies," *Phys. Rev. Lett.*, vol. 95, no. 20, pp. 203 901–4, 2005.
- [15] Th. Koschny, P. Markos, E. N. Economou, D. R. Smith, D. C. Vier, and C. M. Soukoulis, "Impact of the inherent periodic structure on the effective medium description of left-handed and related meta-materials," *Phys. Rev. B*, vol. 71, no. 24, pp. 245 105–22, 2005. [Online]. Available: <http://link.aps.org/abstract/PRB/v71/e245105>
- [16] S. Burger, L. Zschiedrich, R. Klose, A. Schädle, F. Schmidt, C. Enkrich, S. Linden, M. Wegener, and C. M. Soukoulis, "Numerical investigation of light scattering off split-ring resonators," *Proc. SPIE Int. Soc. Opt. Eng.*, vol. 5955, pp. 18–26, 2005.
- [17] C. Enkrich, F. Pérez-Willard, D. Gerthsen, J. F. Zhou, C. M. Soukoulis, M. Wegener, and S. Linden, "Focused-ion-beam nanofabrication of near-infrared magnetic metamaterials," *Adv. Mater.*, vol. 17, no. 21, pp. 2547–2549, 2005.
- [18] A. N. Lagarkov and A. K. Sarychev, "Electromagnetic properties of composites containing elongated conducting inclusions," *Phys. Rev. B*, vol. 53, no. 10, pp. 6318–6336, 1996.
- [19] L. Panina, A. Grigorenko, and D. Makhnovskiy, "Optomagnetic composite medium with conducting nanoelements," *Phys. Rev. B*, vol. 66, no. 15, pp. 155 411–17, 2002.
- [20] V. A. Podolskiy, A. K. Sarychev, E. E. Narimanov, and V. M. Shalaev, "Resonant light interaction with plasmonic nanowire systems," *J. Opt. A: Pure Appl. Opt.*, vol. 7, no. 2, pp. S32–S37, 2005.
- [21] A. N. Grigorenko, A. K. Geim, H. F. Gleeson, Y. Zhang, A. A. Firsov, I. Y. Khrushchev, and J. Petrovic, "Nanofabricated media with negative permeability at visible frequencies," *Nature*, vol. 438, no. 7066, pp. 335–338, 2005.
- [22] G. Dolling, C. Enkrich, M. Wegener, J. F. Zhou, C. M. Soukoulis, and S. Linden, "Cut-wire pairs and plate pairs as magnetic atoms for optical metamaterials," *Opt. Lett.*, vol. 30, no. 23, pp. 3198–3200, 2005. [Online]. Available: <http://www.opticsinfobase.org/abstract.cfm?URI=ol-30-23-3198>
- [23] V. P. Drachev, W. Cai, U. Chettiar, H.-K. Yuan, A. K. Sarychev, A. V. Kildishev, G. Klimeck, and V. M. Shalaev, "Experimental verification of an optical negative-index material," *Laser Phys. Lett.*, vol. 3, no. 1, pp. 49–55, 2006. [Online]. Available: <http://dx.doi.org/10.1002/lapl.200510062>
- [24] S. Zhang, W. Fan, B. K. Minhas, A. Frauenglass, K. J. Malloy, and S. R. J. Brueck, "Midinfrared resonant magnetic nanostructures exhibiting a negative permeability," *Phys. Rev. Lett.*, vol. 94, no. 3, pp. 037 402–4, 2005. [Online]. Available: <http://link.aps.org/abstract/PRL/v94/e037402>
- [25] S. Zhang, W. Fan, K. J. Malloy, S. R. Brueck, N. C. Panoiu, and R. M. Osgood, "Near-infrared double negative metamaterials," *Optics Express*, vol. 13, no. 13, pp. 4922–4930, 2005.
- [26] J. B. Pendry, "Negative refraction makes a perfect lens," *Phys. Rev. Lett.*, vol. 85, no. 18, pp. 3966–3969, 2000. [Online]. Available: <http://link.aps.org/abstract/PRL/v85/p3966>
- [27] R. Merlin, "Analytical solution of the almost-perfect-lens problem," *Appl. Phys. Lett.*, vol. 84, no. 8, pp. 1290–1292, 2004.
- [28] V. A. Podolskiy and E. E. Narimanov, "Near-sighted superlens," *Opt. Lett.*, vol. 30, no. 1, pp. 75–77, 2005.



Stefan Linden obtained his Ph.D. in 2002 at the Physics Department of the Universität Marburg, Germany. Afterwards he received a Feodor Lynen Research Fellowship from the Alexander von Humboldt Foundation and spent one year at the University of Toronto working on the nonlinear properties of photonic crystals. He is currently a post doctoral researcher at the Institute of Nanotechnology at the Forschungszentrum Karlsruhe. Since 2006 he leads a Helmholtz young investigators group. He has a strong background in ultrafast spectroscopy, optics of metal nanostructures, photonic crystals, and electron-beam lithography. His recent research efforts are focused on the nonlinear optical properties of photonic crystals and the realization of left-handed metamaterials for telecommunication wavelengths.



Christian Enkrich received his Diplom in physics at the Universität Karlsruhe (TH) in 2001 with a thesis on the fabrication of three-dimensional Photonic Crystals. Currently he is working towards his Ph.D. degree in physics at the Institut für Angewandte Physik at the Universität Karlsruhe (TH). He has expertise in the fabrication and characterization of metamaterials for the near-infrared wavelength regime and corresponding numerical simulations.



Gunnar Dolling, born in 1982 in Germany, is currently working towards his Diplom in physics at the Universität Karlsruhe (TH) with focus on metamaterials at telecommunication and optical wavelengths.



Costas M. Soukoulis received his B.S. in Physics from Univ. of Athens in 1974. He obtained his doctoral degree in Physics from the Univ. of Chicago in 1978. From 1978 to 1981 he was visiting Assistant Professor at the Physics Dept. at Univ. of Virginia. He spent 3 years (1981-84) at Exxon Research and Engineering Co. and since 1984 has been at Iowa State Univ. (ISU) and Ames Laboratory. He is currently a Distinguished Professor of Physics. He has been an associated faculty member of FORTH since 1983 and since 2001 is a Professor (part-time) at Dept. of Materials Science and Engineering at Univ. of Crete. He has approximately 300 publications, more than 7000 citations and 2 patents for photonic crystals. Prof. Soukoulis is Fellow of the American Physical Society, Optical Society of America, and American Association for the Advancement of Science. He is the senior Editor of the new Journal "*Photonic Nanostructures: Fundamentals and Applications*." His current research interests include photonic crystals, left-handed materials, random lasers, light localizations and theory of disordered systems.



ments with metallic photonic crystals and metamaterials.

Matthias W. Klein received his Diplom in physics from the Universität Heidelberg, Germany, in 2002 and is currently working towards his Ph.D. degree in physics at the Universität Karlsruhe (TH). Between 1999 and 2000, he studied at Cornell University, Ithaca, NY, as a Cornell-Heidelberg Exchange Fellow and contributed to experimental and theoretical research in organic nanoelectronics. He performed his Diplom thesis in the field of quantum optics, before turning to his current area of nanophotonics, where he focuses on linear and nonlinear experiments with metallic photonic crystals and metamaterials.



Jiangfeng Zhou was born in 1976, received his M.S. degree in physics from Beijing University, China, in 2001 and is currently working towards his Ph.D. degree at Iowa State University, USA.



Sven Burger received his PhD. in 2000 from the Physics department of the University of Hannover, Germany, where he was a member of the Institute of Quantum Optics. From 2000 to 2001 he was appointed as post doctoral researcher in an EU TMR network at the European Laboratory for Nonlinear Spectroscopy in Florence, Italy. In 2002 he joined the Numerical Analysis and Modelling group at the Zuse Institute Berlin, Germany, and became a member of the DFG Research Center Matheon, Berlin, in 2003. Since 2004 he is also a member of the spin-off company JCMwave.

S. Burger has a strong background in the field of atom optics where his research includes the observation of solitons in Bose-Einstein condensates and the realization of arrays of Josephson-Junctions in atomic systems. His recent research focuses on developing numerical methods for Maxwell's equations, with applications to photonic crystals, photolithography, metamaterials, and others.



Thomas Koschny, born in July 1971, received his M.Sc. and Ph.D. degrees in physics from the Universität Leipzig, Germany, in 1997 and 2001, respectively. During 2000–2002, he worked as a post-doctoral researcher about Quantum Hall Effect at the Physikalisch-Technische Bundesanstalt Braunschweig (PTB), Germany. Since 2003 he is working about electromagnetic wave propagation in left-handed metamaterials at Institute of Electronic Structure and Laser (IESL) – Foundation for Research and Technology Hellas (FORTH), Crete, Greece.

Since 2004 he is a researcher at Ames Laboratory and Department of Physics and Astronomy at Iowa State University, Iowa, USA. His current research interests include theory of left-handed metamaterials and photonic crystals.



Frank Schmidt received his PhD. (electrical engineering/optical telecommunications) from Humboldt University Berlin, Germany, in 1989, and his habilitation (mathematics) from Free University Berlin in 2002. Since 1992 he is a researcher at Zuse Institute Berlin, where since 1996 he heads the Computational Nano-Optics group. Further, F. Schmidt is one of the scientists in charge of the application area Electronic Circuits and Optical Technologies of the DFG Research Center Matheon and he is one of the founders of the spin-off company JCMwave. He is author and coauthor of about 40 papers in the field of numerical methods in optics.



Martin Wegener obtained his Ph.D. in December 1987 at the Physics Department of the Johann Wolfgang Goethe-Universität Frankfurt. After a postdoc at AT&T Bell Laboratories (Holmdel, U.S.A.) he immediately became an associate professor at the Universität Dortmund in June 1990. Since October 1995, he is a full professor at the Universität Karlsruhe (TH), since 1997 head of the DFG graduate school Collective Phenomena in Solids, since 2001 a group leader at the institute of nanotechnology at the Forschungszentrum Karlsruhe, and since 2001 coordinator of the Karlsruhe DFG-Center for Functional Nanostructures (CFN).

His research interests cover different areas of photonics, such as, e.g., nonlinear-optical spectroscopy, ultrafast spectroscopy, extreme nonlinear optics, near-field optical spectroscopy, photonic band-gap materials, and photonic metamaterials. In 1993 he obtained the Research Award of the Alfried Krupp von Bohlen und Halbach-Stiftung, in 1998 the Teaching Award of the State of Baden-Württemberg, in 2000 the DFG-Leibniz award, and in 2005 the Descartes-Prize of the European Union (together with Costas Soukoulis, Stefan Linden, and others for metamaterial work). He has written two textbooks, has coauthored about 150 publications in peer-reviewed journals and international conferences and has given about 50 invited talks at international conferences. He also serves as referee for a number of national committees and various international journals. Since 2005 he is a topical editor of JOSA B (Journal of the Optical Society of America).